Identification and Isolation of a Hyperphosphorylated, Conformationally Changed Intermediate of Human Protein Tau Expressed in Yeast†

Tom Vandebroek,[‡,§] Thomas Vanhelmont,[‡,||] Dick Terwel,[§] Peter Borghgraef,[§] Katleen Lemaire,[||] Johan Snauwaert,[⊥] Stefaan Wera,[#] Fred Van Leuven,*[,§] and Joris Winderickx[||]

Experimental Genetics Group, Laboratory of Functional Biology, and Laboratory of Molecular and Nanometals, K. U. Leuven, and reMYND NV, B-3000 Leuven, Belgium

Received April 13, 2005; Revised Manuscript Received June 7, 2005

ABSTRACT: Hyperphosphorylation and aggregation of protein tau are typical for neurodegenerative tauopathies, including Alzheimer's disease (AD). We demonstrate here that human tau expressed in yeast acquired pathological phosphoepitopes, assumed a pathological conformation, and formed aggregates. These processes were modulated by yeast kinases Mds1 and Pho85, orthologues of GSK-3β and cdk5, respectively. Surprisingly, inactivation of Pho85 increased phosphorylation of tau-4R, concomitant with increased conformational change defined by antibody MC1 and a 40-fold increase in aggregation. Soluble protein tau, purified from yeast lacking *PHO85*, spontaneously and rapidly formed tau filaments in vitro. Further fractionation of tau by anion-exchange chromatography yielded a hyperphosphorylated monomeric subfraction, termed hP-tau/MC1, with slow electrophoretic mobility and enriched with all major epitopes, including MC1. Isolated hP-tau/MC1 vastly accelerated in vitro aggregation of wild-type tau-4R, demonstrating its functional capacity to initiate aggregation, as well as its structural stability. Combined, this novel yeast model recapitulates hyperphosphorylation, conformation, and aggregation of protein tau, provides insight in molecular changes crucial in tauopathies, offers a source for isolation of modified protein tau, and has potential for identification of modulating compounds and genes.

Protein tau is a microtubule-associated protein (MAP)[1] presumed to stabilize microtubules and to regulate axonal transport in brain. Six isoforms formed by mRNA splicing differ in N-terminal regions and in either three (3R) or four (4R) C-terminal microtubule-binding domains. Binding to microtubules is dynamically regulated by phosphorylation (*1*−*3*), and hyperphosphorylation is thought to contribute to the pathogenesis in a diverse group of tauopathies including Alzheimer's disease (AD) (*4*−*6*). Consequently, phosphorylation of tau by kinases is intensely studied (*1*−*3*). Although tau is a "naturally unfolded protein", conformational changes are detected by specific monoclonal antibodies and could be essential in the formation of aggregates (*7*−*9*), eventually involving heat-shock proteins as chaperones (*10*, *11*). Whether binding to microtubules and aggregation of tau are divergent processes and precisely how they are modulated by phosphorylation and conformation remains to be determined.

Prominent tau kinases are proline-directed protein kinases, e.g., glycogen synthase kinase 3β (GSK-3β) and cyclin-dependent protein kinases (cdk5, cdc2), mitogen-activated and stress-activated protein kinases. Important, non-proline-directed protein kinases are MAP-affinity-regulated kinases, calcium−calmodulin protein kinase II, and protein kinase A (*1*−*3*). Intensely studied are cdk5 and GSK-3β although their exact contribution to and relevance for the pathology is debated, due to their complex regulation in multiple activities in neurons (*7*, *12*−*15*). Conflicting views surround cdk5, a kinase specific for postmitotic neurons and not directly involved in cell cycle control (*13*). The cdk5 catalytic subunit, in association with regulatory subunits p35 (or truncated p25) or p39, can phosphorylate tau in vitro (*16*) and in brain of p25 transgenic mice (*17*) but not in triple transgenic mice expressing tau-4R, cdk5, and p35 (*18*). Decreased cdk5 activity in p35−/− mice paradoxically increased tau phosphorylation at epitopes PHF1/AD2 (*19*).

These considerations incited us to study human protein tau in yeast as a less complex cellular model, as for other aspects of neurodegeneration (*20*−*23*). The yeast orthologue of cdk5, i.e., Pho85 (*24*), is activated by mammalian cyclins as well as p25, and conversely, yeast cyclins activate cdk5 (*25*), demonstrating close functional homology. Although yeast lacks an equivalent of mammalian tau, this was an advantage for our studies since expression of human tau was not competed for nor confounded by an endogenous MAP

† This investigation was supported by the Fonds voor Wetenschappelijk Onderzoek-Vlaanderen (FWO-Vlaanderen), KULeuven Special Research Fund (KULeuven-BOF), Instituut voor Wetenschappelijk en Technisch Onderzoek (IWT), KULeuven R&D, and the Roomsfund.

* Corresponding author: tel, +32 16 34 58 88; fax, +32 16 34 58 71; e-mail, fredvl@med.kuleuven.ac.be.

‡ Contributed equally to this work.

§ Experimental Genetics Group.

|| Laboratory of Functional Biology.

⊥ Laboratory of Molecular and Nanometals.

reMYND NV.

[1] Abbreviations: cdk5, cyclin-dependent protein kinase 5; cdc2, cell division cycle 2; DMSO, dimethyl sulfoxide; GSK3β, glycogen synthase kinase 3β; MAP, microtubule-associated sulfate protein; SDS, sodium dodecyl sulfate; PAGE, polyacrylamide gel electrophoresis; PKA, protein kinase A; TBS, Tris-buffered saline.

10.1021/bi0506775 CCC: $30.25
Published on Web 08/04/2005

as is the case in mammalian cells and in transgenic mice (*14*, *26*).

We demonstrate here that events from phosphorylation to aggregation of tau are recapitulated in yeast, i.e., formation of a tau fraction enriched in phosphoepitopes and in the conformational epitope MC1. This form is proposed to be directly involved in tau aggregation, as corroborated after its isolation, forming aggregates as in the brain of transgenic mice (*26*). Mds1, an orthologue of GSK-3β, was the major yeast proline-directed tau kinase, but unexpectedly, Pho85 exerted negative regulation, corroborating recent observations in mammalian systems (*19*). Combined, the recapitulation of hyperphosphorylation, conformation, and aggregation in yeast cells as demonstrated allow analysis of fundamental mechanisms that act on human protein tau in this cellular model.

EXPERIMENTAL PROCEDURES

Strains and Culture Conditions. Yeast strains were isogenic to wild-type strains BY4741 (Mat a *his*3D1 *leu*2D0 *met*15 D0 *ura*3D0) (*27*) and W303-1A (Mat a *leu*2-3 112 *ura*3-1 *trp*1-1 *his*3-11 15 *ade*2-1 *can*1-100 *GAL SUC*) (*28*). Deletion of *MDS1* and *PHO85* was by replacement of corresponding coding regions with PCR-derived KanMX cassettes in BY4741 strain or with *HIS3* or *TRP1* cassettes in W303-1A strain (*29*). cDNA coding for human tau isoforms 2N/4R and 2N/3R (*30*) were inserted in episomal plasmid pYX212 under control of the strong constitutive *TPI1* promoter (R&D Systems, Minneapolis, MN). Human GSK-3β[S9A] cDNA (*31*) was inserted with a KanMX-resistance cassette in a pUG6-based vector (*32*). Yeast transformants (*33*) were selected for growth on minimal selective medium (*34*). Cultures were grown at 30 °C in glucose-containing minimal medium lacking uracil until early exponential phase (OD_{600} $\sim$ 2). Cells were collected by centrifugation and stored at −70 °C until further analysis.

Western Blotting and Silver Staining. Yeast cells were lysed by boiling for 15 min in SDS sample buffer [50 mM Tris (pH 8.0), 10 mM β-mercaptoethanol, 2% SDS, 0.1% bromophenol blue, 10% glycerol] for SDS−PAGE. For native PAGE, cells were resuspended in ice-cold TBS, homogenized, and centrifuged for 2 h at 150000*g* at 4 °C; the supernatant was mixed with 100 mM Tris (pH 8.6), 0.005% bromophenol blue, and 10% glycerol for analysis. After separation by SDS−PAGE or by native PAGE on 8% or 4−20% Tris−glycine gels (Invitrogen, Carlsbad, CA), proteins were transferred to nitrocellulose membranes (Hybond-C; Amersham, Buckinghamshire, U.K.) for western blotting (*35*) or silver staining (Amersham, Buckinghamshire, U.K.).

Antibodies. Primary antibodies used with their specificity: Tau-5, all tau isoforms (Pharmingen, San Jose, CA); AD2, P-S396/P-S404 (VCDN, Lille, France); AT8, P-S202/P-S205; AT100, P-T212/P-S214; AT180, P-T231/P-S235; AT270, P-T181 (Innogenetics, Gent, Belgium); PG5, P-S409 and MC1, conformational epitope (gifts from P. Davies). Immunoreactions were quantified after densitometric scanning (Imagemaster1D software; Amersham, Buckinghamshire, U.K.) and always normalized for the total amount of tau determined by blotting with the Tau-5 pan-tau antibody. The relative amount of sarkosyl-insoluble tau was determined by western blotting with antibody Tau-5 and normalized for soluble tau.

Isolation of Sarkosyl-Insoluble Tau Aggregates. Pelleted cells were resuspended in TBS (25 mM Tris, pH 7.7, 150 mM NaCl) containing protease inhibitor cocktail (Roche, Darmstadt, Germany) and 0.25 mM PMSF, 5 μg/mL TLCK, 5 μg/mL TLPCK, 5 mM EDTA, 100 mM NaF, 10 μM okadaic acid, and 0.2 mM sodium vanadate. Cells were homogenized, the concentrations of NaCl and sucrose of the supernatant were adjusted to 0.8 M and 10% (w/v), respectively, and after centrifugation (20000*g*, 30 min; 4 °C) *N*-lauroylsarkosine (Sigma, St. Louis, MO) was added to the supernatant [final concentration 1% (w/v)]. After incubation for 1 h at 4 °C and centrifugation (150000*g*, 40 min; 4 °C) the pellet and supernatant were stored at −20 °C for analysis.

Purification of Tau-4R. Collected yeast cells were frozen in liquid nitrogen, ground with sterile sand (Sigma, St. Louis, MO), and resuspended in 100 mM MES (pH 6.8) with 1 mM β-mercaptoethanol, protease inhibitor cocktail (Roche, Darmstadt, Germany), 2.5 mM PMSF, 5 μg/mL TLCK, 5 μg/mL TLPCK, 5 mM EDTA, 100 mM NaF, 10 μM okadaic acid, and 0.2 mM sodium vanadate. After centrifugation (20000*g*, 30 min; 4 °C), the supernatant was boiled for 10 min and centrifuged (20000*g*, 30 min; 4 °C). The extracted proteins were resolved by anion-exchange chromatography (HiTrap Q; Amersham Biotech, Amersham, U.K.) and eluted with a three-step salt gradient (0−0.2, 0.2−0.3, and 0.3−1 M NaCl). Fractions were analyzed by spot test or western blotting with Mab tau-5, and fractions containing tau were pooled and concentrated using 10 kDa centricon devices (Millipore).

In Vitro Aggregation of Tau-4R. Protein tau, isolated from different yeast strains as specified, was incubated (0.3 μM) at 37 °C for 2 h in buffer containing 50 mM MES (pH 6.8) and 150 mM NaCl. After centrifugation (150000*g*, 1 h; 30 °C) pellets were resuspended in 50 mM MES (pH 6.8) and either fixed with 2% glutaraldehyde for electron microscopy or, for atomic force microscopy, deposited on silanized silicon supports (*26*). Low-power images were taken with Point probes type FM cantilevers (Nanoworld, Neuchatel, Switzerland) while high-power images were obtained with Data probe type cantilevers (DP18/HI′RES/AIBS) (Mikro-Masch, Madrid, Spain). Tau aggregates were quantified by SDS−PAGE and western blotting with Mab Tau-5 (*26*).

Statistical Analysis. Statistical analysis was performed by one-way or two-way ANOVA on logarithmically transformed data, followed by the multiple comparison test of Tukey.

RESULTS

Human Protein Tau-4R Becomes Hyperphosphorylated in Yeast. Human tau-4R and tau-3R isoforms, which were expressed in wild-type yeast strains BY4741 (Figure 1A, lanes 1) and W303-1A (data not shown), did not affect growth rate of any yeast strains used in this study (results not shown). Western blot analysis with the pan-tau antibody Tau-5 of total protein extracts demonstrated that tau-4R migrates as a set of proteins of apparent M_r 64−72 kDa (Figure 1A, upper panels, lanes 1) and tau-3R as 60−68 kDa proteins (Figure 1A, lower panels, lanes 1). Alkaline phosphatase treatment reduced the tau-3R and tau-4R subspecies to single proteins of 60 and 64 kDa, respectively (results not shown).

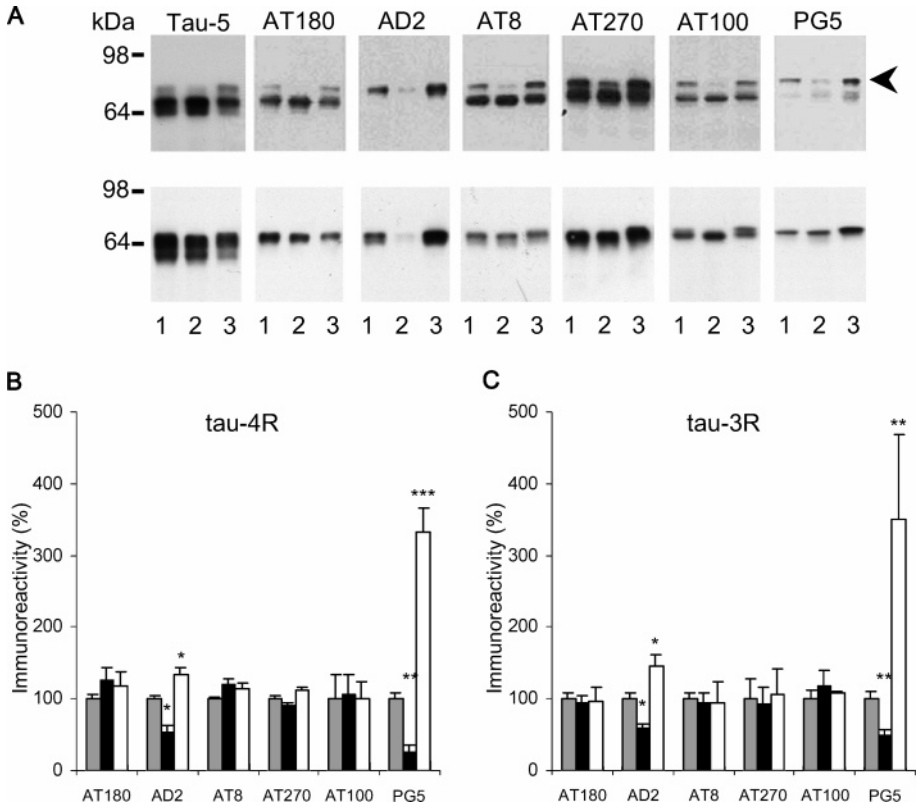

FIGURE 1: Phosphoepitope mapping of human protein tau-3R and tau-4R expressed in yeast. (A) Western blotting with Mabs indicated of total extracts of tau-4R (upper panel) and tau-3R (lower panel) expressed in wild-type (lanes 1), *mds1*Δ (lanes 2), and *pho85*Δ (lanes 3) yeast strains. The arrowhead on the right denotes slow-mobility hyperphosphorylated tau (hP-tau). (B, C) Relative levels of different epitopes on tau-4R (B) and tau-3R (C) in wild-type (gray bars), *mds1*Δ (black bars), and *pho85*Δ (open bars) yeast strains. Apparent molecular mass in kDa is indicated on the left. Data are the mean with SEM of three independent experiments. Asterisks denote statistically significant differences (*, $p < 0.05$; **, $p < 0.01$; ***, $p < 0.001$).

Epitope mapping defined three to four distinctly migrating phosphorylated subspecies, differentially reacting with antibodies AD2, AT8, AT180, AT270, AT100, and PG5 (Figure 1A), some reacting strongly with a slow migrating subspecies of tau-4R (Figure 1A, upper panels, arrowhead). Significantly, Mab AD2 reacted nearly exclusively and Mab PG5 predominantly with this slow-migrating tau-4R species, further referred to as hyperphosphorylated tau (hP-tau). Importantly, the relatively weak reaction of pan-tau antibody Tau-5 with this hP-tau species indicated its lower abundance in mass as opposed to its strong reaction with Mabs that define pathological epitopes (AD2, AT8, AT270, AT100, PG5).

The clear demonstration of hyperphosphorylation of tau-4R encouraged us to develop yeast further as a cellular model. Although the combined phosphorylation could explain the slow electrophoretic migration of hP-tau, the distinct and abrupt change to slow mobility was most conspicuously marked by the AD2 epitope, i.e., phosphorylation at serine residues S396/S404. Since this is a typical GSK-3β substrate site, we examined the yeast kinases that are equivalent to GSK-3β, besides the orthologue of cdk5, as these were the first demonstrated mammalian tau kinases.

Opposite Effects of Yeast Kinases Mds1 and Pho85 on Tau Phosphorylation and MC1 Conformation. To define the observed phosphoepitopes, particularly AD2, we expressed human protein tau in yeast cells deficient in Mds1, an orthologue of mammalian GSK-3β. As expected, the AD2 epitope on tau-3R and tau-4R was reduced when quantified over all phosphorylated subforms in BY4741 yeast strain

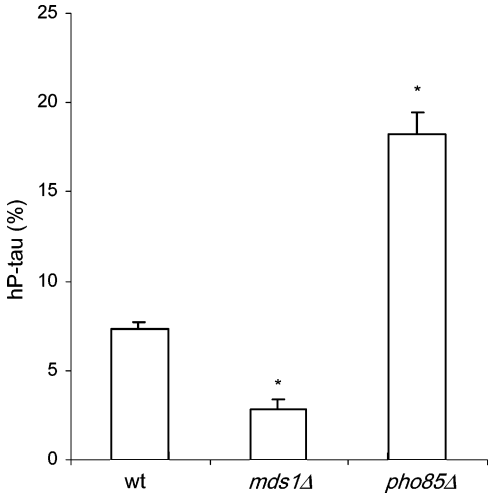

FIGURE 2: Relative levels of hyperphosphorylated tau (hP-tau). Relative levels of hyperphosphorylated tau-4R expressed in wild-type (wt), *mds1*Δ, and *pho85*Δ yeast strain by western blotting with Mab Tau-5 (see Figure 1).

(Figure 1) and in W303 yeast strain (results not shown). Significantly, absence of Mds1p also significantly reduced the PG5 epitope, as well as the amount of slow, hyperphosphorylated hP-tau (Figures 1 and 2). That Mds1 is the yeast kinase responsible for formation of AD2 and PG5 epitopes was further substantiated by complementation of *mds1*-deficient cells with human, constitutively active GSK-3β-[S9A] (*35*) (Figure 3). Moreover, expression in yeast strains deficient in other GSK-3β orthologues, i.e., Mck1, Mrk1,

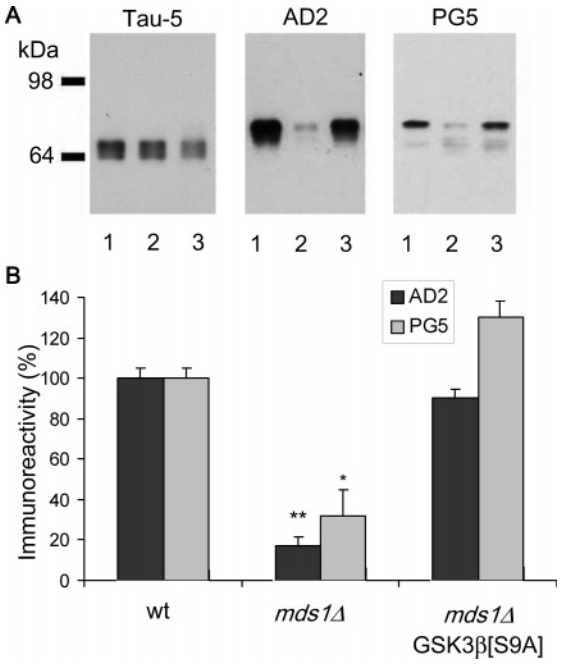

FIGURE 3: Decrease of epitopes AD2 and PG5 in *mds1*Δ yeast is restored by human GSK-3β[S9A]. Western blots (A) and relative levels (B) of AD2 (black bars) and PG5 (gray bars) on tau-4R in wild type (wt) (lanes 1), *mds1*Δ yeast cells (lanes 2), and *mds1*Δ cells expressing human GSK-3β[S9A] (lanes 3). Data are normalized for total tau-4R present determined with pan-tau Mab Tau-5 (A, left panel). Depending on the exposure to film, hP-tau bands that react strongly with AD2 and PG5 are faint on western blots with Tau-5 (compare with Figure 1). Data are the mean with SEM of three independent experiments. Asterisks denote statistically significant differences (*, $p < 0.05$; **, $p < 0.01$).

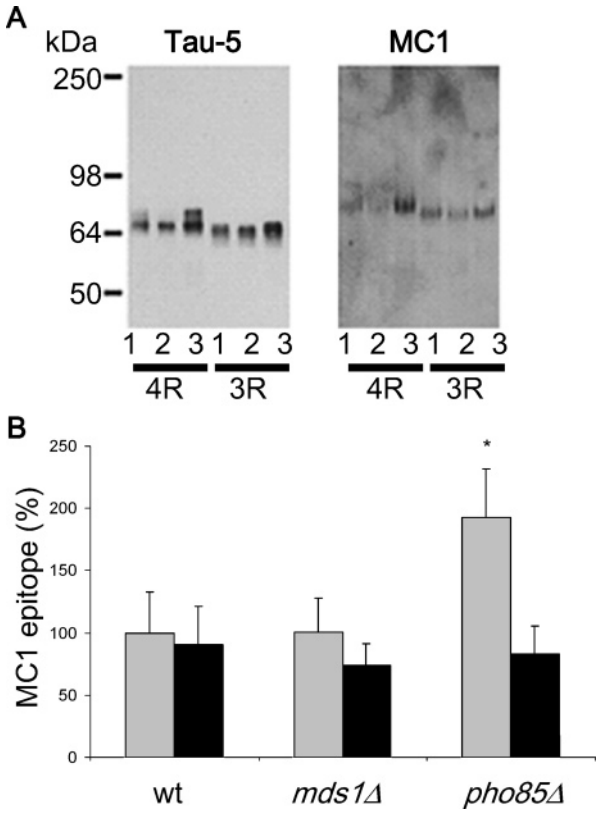

FIGURE 4: Conformation defined by Mab MC1 is increased in *pho85*Δ cells. (A) Soluble tau-4R and tau-3R in wild-type (lanes 1), *mds1*Δ (lanes 2), and *pho85*Δ (lanes 3) yeast strains blotted after SDS−PAGE with Mab Tau-5 (left panel) or native PAGE with Mab MC1 (right panel). (B) Relative levels of epitope MC1 on tau-4R (gray bars) and tau-3R (black bars) in wild-type, *mds1*Δ, and *pho85*Δ yeast strains. All data are normalized for total amount of tau determined with Tau-5 and are the mean with SEM of three independent experiments. The asterisk denotes statistically significant difference ($p < 0.05$).

and Yol128c, affected much less or not at all the phosphorylation of human protein tau at these epitopes (results not shown). The restoration of both AD2 and PG5 epitopes to levels approaching or even superseding those in wild-type yeast by complementation with GSK-3β[S9A] (Figure 3) complied fully with our observations in brain of double transgenic mice, coexpressing human tau-4R and GSK-3β, in which the AD2 epitope was also most affected (*35*).

We went on to similarly express human tau-3R and tau-4R in yeast cells lacking Pho85p, the orthologue of cdk5, and another major mammalian tau kinase. Unexpectedly, phosphorylation of tau was dramatically increased for epitope PG5 and, to a lesser extent, epitope AD2 (Figure 1A, lanes 3). Moreover, the amount of hP-tau was significantly increased to reach nearly 20% of all cellular tau present (Figure 2). Concomitantly, increased reaction with the conformation-dependent antibody MC1 was demonstrated by western blotting after native gel electrophoresis, which was most evident for tau-4R in yeast cells lacking Pho85 (Figure 4; see also further below).

The data demonstrated that, in contrast to Mds1, Pho85 contributed negatively to the phosphorylation of human tau mainly at epitopes PG5 and AD2, which are typical substrate sites for protein kinase A and GSK-3β, respectively (*7*, *12*, *36*, *37*). Moreover, hyperphosphorylation in the absence of Pho85p favored induction of the conformation recognized by antibody MC1, a marker for pathological tau filaments and their precursors (*9*, *38*).

Inactivation of Yeast Kinase Pho85 Increased Sarkosyl-Insoluble Tau Aggregates. The occurrence of the MC1 epitope in addition to the other pathological epitopes, PG5, AD2, and AT100, prompted us to comparatively measure the amount of sarkosyl-insoluble tau in wild-type, *mds1*Δ, and *pho85*Δ strains.

In wild-type yeast, human tau-3R and tau-4R consistently formed sarkosyl-insoluble tau as a small but reproducible fraction of total tau present (Figure 5A,B). Inactivation of Mds1p did not significantly affect aggregation of either tau isoform (Figure 5A,B). In contrast, deficiency of *pho85* dramatically increased sarkosyl-insoluble tau levels by about 40-fold for tau-4R, denouncing an outspoken isoform contribution since only about a 3-fold increase was observed for tau-3R (Figure 5C,D). These quantitative observations were consistent in independent transformations and independent experiments, resulting in highly significant statistical differences for tau-4R expressed in the *pho85*-deficient yeast, for these and other parameters analyzed (Figures 1−5).

Western blotting of isolated sarkosyl-insoluble aggregates with different Mabs revealed that phosphoepitopes were present but differentially distributed on soluble and insoluble protein tau. Most notable were epitopes AT100 and PG5, present highly enriched in the sarkosyl-insoluble tau-fractions isolated from *pho85*-deficient yeast cells (Figure 5E). Since both epitopes were also present on hP-tau, the slow migrating hyperphosphorylated form of tau-4R (Figures 1 and 5E), this molecular form of tau is hereby identified as intricately linked

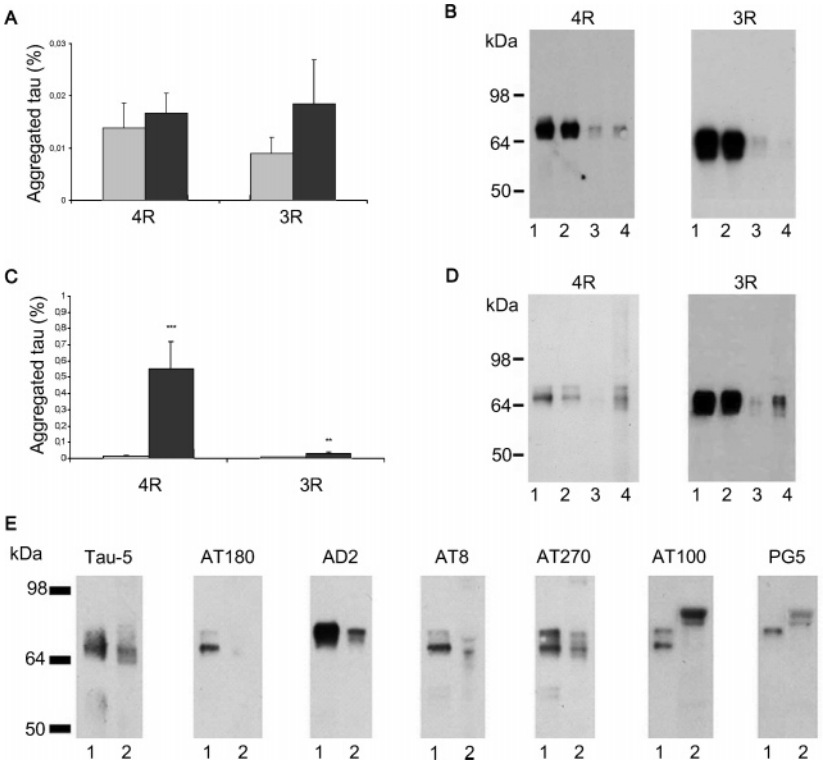

FIGURE 5: Isolation and quantification of sarkosyl-insoluble tau. (A) Aggregates of protein tau-3R and tau-4R, insoluble in sarkosyl (1%), in wild-type (gray bars) or *mds1*Δ (black bars) yeast. (B) Western blot with Tau-5 of soluble (lanes 1 and 2) and sarkosyl-insoluble (lanes 3 and 4) extracts from wild-type (lanes 1 and 3) and *mds1*Δ yeast (lanes 2 and 4) expressing either tau-4R (left panel) or tau-3R (right panel). (C) Insoluble aggregates of protein tau-3R and tau-4R in wild-type (gray bars) or *pho85*Δ (black bars) yeast. Note the difference in ordinate. (D) Western blot with Tau-5 of soluble (lanes 1 and 2) and sarkosyl-insoluble (lanes 3 and 4) extracts from wild-type (lanes 1 and 3) and *pho85*Δ yeast (lanes 2 and 4) expressing either tau-4R (left panel) or tau-3R (right panel). Note that more sarkosyl-insoluble than soluble tau was loaded (see Experimental Procedures section) while western blots with tau-3R were longer exposed than tau-4R to visualize sarkosyl-insoluble tau aggregates. (E) Western blotting of soluble (lanes 1) and sarkosyl-insoluble tau (lanes 2) from tau-4R in *pho85*Δ yeast. Note the difference in mobility that is extra highlighted due to differential reaction with the antibodies and to the loading of higher amounts of sarkosyl-insoluble aggregates (see Experimental Procedures section and legend to Figure 4). All data are the mean with SEM of thtree independent experiments. Asterisks denote significant differences (**, $p < 0.05$; ***, $p < 0.001$).

to, or even responsible for, the accumulation of sarkosyl-insoluble tau aggregates. Western blotting with Tau-5 demonstrated, on the other hand, that hP-tau did not make up the bulk of the aggregates (Figure 5E), an apparent contradiction that was further explored and clarified by analysis of the isolated tau fractions (see below).

Combined, the data extend the negative contribution of the yeast kinase Pho85 from the increase in phosphorylation at epitopes PG5 and AD2 to the increased conformational change defined by MC1 and further to the increased formation of intracellular aggregates. Since this sequence of events covers the pathogenic spectrum proposed in tauopathies, the yeast model was further characterized with emphasis on Pho85.

Purification of Total Tau and Hyperphosphorylated Tau. For further structural and functional characterization of the aggregation process, we developed a method to isolate tau from wild-type and deficient yeast strains to obtain specified pre- and posttranslationally modified human protein tau. Yeast appears well suited for this goal, which cannot be attained by bacterial expression systems. The resulting isolation method was essentially based on heat treatment of total extracts, prepared in the presence of high concentrations of proteinase and phosphatase inhibitors, followed by anion-exchange chromatography (Figure 6A). The procedure enabled rapid purification of human protein tau from yeast strains in relatively high yields (20 μg of tau from 1 L cultures) and with a relatively high recovery (10−15%). Quality control by western blotting and silver staining demonstrated the final preparations to contain predominantly human tau (between 90% and 97%) with only minor amounts of degradation products (Figure 6B,C).

Human protein tau-4R expressed in and isolated from wild-type, *mds1*-deficient and *pho85*-deficient yeast cells showed very similar patterns of epitopes as the respective total homogenates (Figure 6C, compare to Figure 1A). Significantly, the isolates contained also the slow-migrating hP-tau species in a very similar relative abundance as in the original total yeast extracts (Figure 6C). The overall isolation procedure was thereby validated to yield purified protein tau-4R that was indistinguishable from, and representative for, the yeast intracellular tau-4R protein. By alterations in the anion-exchange elution gradient profile, further separation into subfractions with different electrophoretic mobility was achieved. Particularly, the fractions of tau-4R eluting at higher salt concentrations (Figure 6A, dashed bar) migrated electrophoretically identical to the slow-mobility hP-tau species described above and retained the pathological phosphoepitopes when examined by western blotting after denaturing PAGE (Figure 6D). Moreover, analysis by native PAGE and western blotting further and directly demonstrated the presence of the MC1 conformational epitope on the purified hP-tau fraction (Figure 6D, right panel).

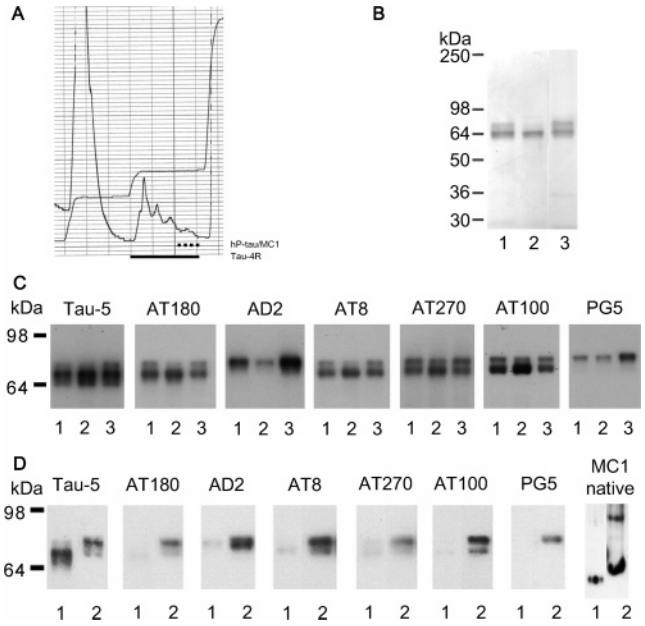

FIGURE 6: Characterization of purified tau-4R and hP-tau. (A) Anion-exchange chromatography of tau-4R expressed in *pho85*Δ yeast, using a three-step salt gradient (tracing from 0 to 1 M NaCl; see also Experimental Procedures section). Elution profile of total proteins as indicated by tracing of OD at 280 nm. Tau-4R eluted between 0.2 and 0.3 M NaCl (indicated by solid bar) and hP-tau/MC1 between 0.24 and 0.3 M NaCl (indicated by dashed bar). (B) Pooled fractions of tau-4R isolated from wild-type (lane 1), *mds1*Δ (lane 2), or *pho85*Δ yeast (lane 3) separated on 4−20% Tris−glycine SDS−PAGE to show purity by silver staining. (C) Pooled fractions of tau-4R isolated from wild-type (lanes 1), *mds1*Δ (lanes 2), and *pho85*Δ yeast (lanes 3) blotted after SDS−PAGE with Mabs indicated. (D) Anion-exchange chromatography fractions eluting at lower salt concentrations (lanes 1) and at higher salt concentrations (lanes 2) (dashed line in panel A) analyzed by SDS−PAGE and western blotting with Mabs indicated and by native PAGE and blotting with Mab MC1 (utmost right panel). Note that native PAGE was subject to some interference by salt present in the sample. M_r markers of SDS−PAGE (shown on the left) do not apply for the native gel.

The combined data demonstrate the very close relation of hyperphosphorylation of tau, the slow electrophoretic mobility, and the induction of conformational changes. This subspecies of hyperphosphorylated protein tau is presumed to represent the pathological predecessor of tau fibrils, and its physical isolation will allow further characterization in structural and functional detail.

Promotion of Aggregation by Hyperphosphorylated Tau in Vitro. Different preparations of protein tau, isolated as total fractions from different transformed yeast strains, were tested for aggregation in vitro by measuring the amounts of aggregated tau by western blotting of high-speed centrifugation pellets, in combination with morphological analysis by electron microscopy and atomic force microscopy.

Total tau-4R fractions isolated from *pho85*Δ yeast cells aggregated about 4 times faster than similar isolates from wild-type or *mds1*Δ yeast cells, tested at the same initial concentrations (Figure 7A,B), thereby corroborating the in vivo observation of increased sarkosyl-insoluble tau aggregation in the *pho85*-deficient yeast cells (Figure 5B,C). The inherent hypothesis that the soluble MC1-reactive hP-tau species was essential for seeding and/or propagation of the polymerization of tau was then tested directly. Aggregation of wild-type tau-4R isolated from wild-type yeast was indeed increased considerably by seeding with very low concentrations (8 nM) of the isolated MC1-reactive hP-tau form (Figure 7A,B).

The tau aggregates present in the high-speed pellets were examined morphologically by electron and atomic force microscopy and were demonstrated to consist of structured tau filaments with a twisted, somewhat irregular appearance of all filaments that differed mainly in length (Figure 7C,D). Sarkosyl-insoluble fractions obtained from total yeast cell extracts were not pure enough for detailed morphologic analysis by electron or atomic force microscopy.

Combined, the experiments demonstrated the ability of yeast cells to hyperphosphorylate human protein tau, conferring conformational alterations that drive aggregation of tau in the yeast cells and after biochemical isolation. Besides these different yeast strains that can be further exploited as informative cellular models, the rapid isolation of hyperphosphorylated tau species will eventually allow elucidation of its salient structural and functional details.

DISCUSSION

Phosphorylation of protein tau controls its normal interaction with microtubules, while hyperphosphorylation is thought to cause or contribute to the aggregation of tau into filaments and tangles in the brain of patients with AD and other tauopathies. As yet, we do not understand the fundamental control mechanisms involved, mainly because tau can be phosphorylated at more than 30 different sites by a wide variety of kinases. Moreover, active mammalian tau kinases, such as GSK-3β and cdk5, are subject to complex regulation by different subunits and interacting proteins, which in turn are regulated by phosphorylation in response to divergent and often opposite signals. Finally, the inherent complexity of neurons hinders the direct definition of the role of kinases in the dynamic functional regulation of tau and its interaction with microtubules. Studying these problems in brain in vivo is an even more daunting task (*18*, *19*, *23*, *26*, *35*). For all of these reasons we examined yeast cells as a less complex model to study the phosphorylation of human protein tau by endogenous yeast kinases.

Phosphorylation of Tau in Yeast. In yeast, human tau-3R or tau-4R isoforms were demonstrated here for the first time to acquire phosphoepitopes that are considered pathological markers in mammalian brain and cells (*7*, *39*, *40*). AT100 is a marker for PHF (*1*−*3*) and can be reconstituted in vitro by isolated GSK-3β and PKA (*7*), while AD2 is a typical GSK-3β epitope marker in tauopathies (*2*). The nonlinear epitope defined by antibody MC1 is highly dependent on the conformation of protein tau (*9*, *41*) and is an excellent marker for PHF and their pathogenic precursors in human brain, as well as in transgenic mouse brain (*9*, *26*, *37*, *38*, *41*, *42*). These observations of specific phosphorylations prompted us to develop yeast as a model system, as reported here.

The deletion of *mds1* and complementation by GSK-3β demonstrated directly that Mds1 is the closest relative to human GSK-3β among its four orthologues in yeast (*43*). Particularly, phosphorylation at S396/S404 (AD2 epitope) corroborates it as the most typical GSK-3β target also in yeast, as in mouse brain (*30*, *35*, *39*). Tau-S409 (PG5 epitope) is not a typical substrate of GSK-3β but of PKA (*7*, *12*, *36*,

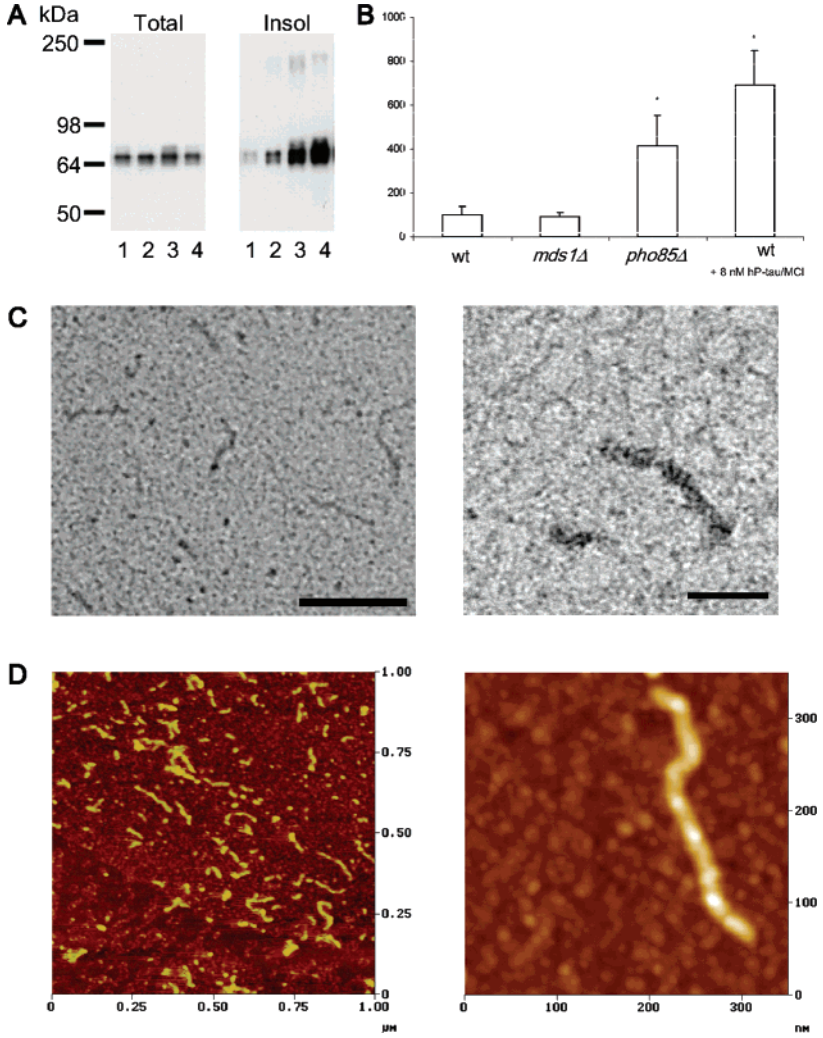

FIGURE 7: In vitro assembly of isolated tau-4R and analysis by EM and AFM. (A) Tau-4R aggregates isolated by centrifugation (right panel) after in vitro formation at 37 °C for 2 h of total tau-4R (left panel) isolated from wild-type (lanes 1), *mds1*Δ (lanes 2), or *pho85*Δ (lanes 3) yeast. In addition, tau-4R isolated from wild-type yeast was spiked with isolated hP-tau (lanes 4), and the aggregates formed were analyzed by western blotting with pan-tau antibody Tau-5. (B) Relative levels of tau aggregates formed in vitro as shown in panel A. Data are the mean with SEM of three independent experiments (asterisks denote statistically significant difference at $p < 0.05$). (C, D) Filaments assembled in vitro from tau-4R from *pho85*Δ yeast visualized by transmission electron microscopy (C) (left panel, scale bar 250 nm; right panel, scale bar 50 nm) and by atomic force microscopy (D) (see Experimental Procedures section).

37), and Mds1 must therefore affect its phosphorylation indirectly. Prephosphorylation by Mds1 could be a requisite for the action of PKA and perhaps also a change in conformation, as suggested by the fact that the PG5 and AD2 epitopes are mainly carried by slow-migrating hP-tau.

Deficiency of yeast *pho85* resulted in three effects that thereby are demonstrated to be intimately related: (i) increased phosphorylation at PG5 and AD2 epitopes, (ii) more tau converted into the MC1 conformation, and (iii) vastly increased sarkosyl-insoluble tau aggregates. Combined, the data support the hypothesis that cdk5 in mammalian neurons (*19*) and Pho85 in yeast (this study) do not phosphorylate tau directly but act indirectly as negative regulators of phosphorylation and, thereby, of conformation and aggregation. Yeast Pho85 is involved in many physiological processes, e.g., nutrient sensing, stress adaptation, cell wall integrity, and glycogen storage (*44*, *45*). Therefore, deletion of pho85 results in multiple phenotypic effects (*46*, *47*), making it difficult to define a specific cause of the observed modifications on protein tau in this study. Despite the vast and obvious differences between yeast cells and neurons, remarkable similar mechanisms appear to regulate cdk5 in neurons and Pho85 in yeast. As an example, inhibition of cdk5 in cultured neurons affected phosphoproteins involved in related processes as inhibition of Pho85 in yeast (*48*). In addition, deletion of Pho85 in yeast cells (this study) and inhibition of cdk5 by p35 inactivation in mice (*19*) both affect phosphorylation of protein tau.

Mds1 is proposed as a prime candidate for negative regulation by Pho85, since essentially the same phosphoepitopes, i.e., PG5 and AD2, were affected by deletion of either Mds1 or Pho85, although in opposite directions. However, Pho85 can phosphorylate Glc8, the orthologue of mammalian inhibitor 2, which controls the activity of Glc7, the orthologue of mammalian protein phosphatase 1 (*49*). Phosphatase 1 dephosphorylates GSK-3β at serine-9, well-known to regulate its activity (*50*), but no comparable regulation of Mds1 in yeast has been observed. On the other hand, deletion of Pho85 alters the expression of several proteins, e.g., mitogen-activated protein kinases Bck1 and Slt2/Mpk1, the PAK kinase Cla4 involved in budding (*51*), and Bem2, a Rho-GTPase-activating protein involved in cell

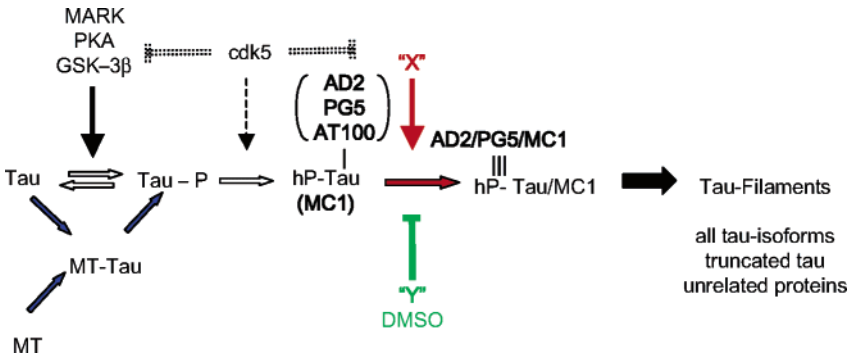

FIGURE 8: Scheme of modifications of human protein tau-4R expressed in yeast. The reversible phosphorylation of tau by different kinases, mammalian as indicated for clarity or their yeast counterparts, causes hyperphosphorylation of tau (hP-tau) at several pathological epitopes (AT100, AD2, PG5). The form "locked" into the conformation defined by MC1 is proposed to be essential in seeding or nucleating the aggregation of tau. Other tau isoforms that are present, or truncated tau or even unrelated proteins, can become incorporated in the filaments. The central step from hyperphosphorylated (hP-tau) to conformationally changed tau (hP-tau/MC1) is subject to positive and negative control (indicated by X and Y). Microtubules (MT) are included for the sake of completeness although yeast MT are not known to bind human protein tau.

polarity (*52*). Some of these could also operate as effectors of tau phosphorylation. Fortunately, these and other types or mechanisms of control can be much more easily addressed in the yeast model than in mammalian cell models.

Conformational Change and Aggregation of Tau in Yeast. Aggregation of tau-4R was greatly promoted by low concentrations of the conformationally altered hyperphosphorylated tau fraction without any further additions. Aggregation of underphosphorylated unfolded protein tau in vitro is slow and requires the addition of cofactors that appear to be necessary to induce aggregation, probably by promoting the induction of an intermediate folded tau species (*53*−*55*). We propose that hP-tau/MC1 is the biochemically stable form of tau that is the actual seed or nucleation factor that initiates and promotes the aggregation of tau. This hypothesis will need further substantiation by more extensive studies aiming (i) to unravel the structure of the conformationally altered hP-tau/MC1 or at least the structure of the MC1 epitope, (ii) to understand kinetically the contribution of the conformationally altered hP-tau/MC1 in promoting in vitro filament formation of underphosphorylated tau-4R, and (iii) to define the mechanism by which hP-tau/MC1 promotes aggregation, either by nucleation only or also by imposing, in a prion-like fashion, its structure onto other tau molecules. This latter highly hypothetical capacity of hP-tau/MC1 could be reflected in the composition of the sarkosyl-insoluble fractions that consist of less phosphorylated tau species besides the hyperphosphorylated tau, but in a distorted ratio. This will need careful qualitative and quantitative analysis by other methods.

The close combination of hyperphosphorylation, conformation, and aggregation and their consistent similar modulation intrinsically by the kinases Mds1 and Pho85 underline their close connection in the proposed sequence of events, schematically represented in Figure 8. The major rate-determining step appears to be the conversion of hyperphosphorylated tau to the MC1 configuration. This step is likely controlled by cytosolic or membrane-associated proteins including chaperones, while also the binding of tau to microtubules would slow the aggregation process by decreasing the concentration of free tau. Factors that accelerate (X-type) or inhibit (Y-type) the conformational conversion will need to be identified, for which this yeast model is well suited. We have identified DMSO as a powerful negative effector of the conformational conversion of tau in vivo, when added at low concentrations during culture (less than 1%). Since DMSO affects the expression of many cytosolic components (*56*), the preliminary results of this observation are not included in this study.

It is tempting to relate or extrapolate the findings in yeast to our observations in parallel studies of different tau transgenic mouse models (*26*). The rate-limiting step defined above, i.e., formation of hP-Tau(MC1) (Figure 8), apparently cannot be overcome in tau-4R transgenic mice, since these do not develop tau filaments, not even when tau is extra-phosphorylated in tau-4R × GSK-3β double transgenic mice (*35*). Only FTD-mutant tau transgenic mice develop tauopathy as in FTD patients (*26*), demonstrating that mutations confer another negative characteristic on tau-4R in this respect, e.g., decreasing binding to microtubules, an aspect being studied in the yeast model. The high nucleation capacity of hP-tau/MC1 would explain the spatial and temporal colocalization of markers of hyperphosphorylation, conformation, and filaments in brain of tau[P301L] transgenic mice during the entire disease process (*26*).

Differences in Tau-3R and Tau-4R Isoforms Are Recapitulated in Yeast. The major contribution of Mds1, i.e., formation of the slow-migrating hyperphosphorylated tau, acted mainly on the tau-4R isoform, on which our efforts were concentrated since it is most important in normal adult brain and in tauopathies (*1*−*3*). Nevertheless, although tau-4R and tau-3R appeared to be phosphorylated to a similar overall extent in yeast, neither pronounced conformational change nor extensive aggregation was detected for tau-3R. This supports in vitro evidence for the second microtubule-binding domain in β-pleated sheet formation and aggregation of tau-4R (*57*) and corroborates the finding mainly of tau-4R in tauopathies (*1*−*3*). The data implicate the second microtubule-binding domain as an essential parameter for tau aggregation, also in yeast cells, although binding of tau to yeast microtubules has, to our knowledge, not been reported.

In conclusion, for the first time yeast is presented as a new cellular model for the analysis of physiological and pathological aspects of human protein tau and as a source for isolation of modified tau, particularly the conformation-

ally stable intermediate form. We identify Mds1 and Pho85 as the yeast kinases that govern in opposite directions the hyperphosphorylation, conformational alterations, and aggregation of tau. The different yeast strains will be further exploited as informative cellular models, while the rapid isolation procedure and the analysis of the isolated hyperphosphorylated tau species will allow the elucidation of their structural and functional details. The mechanisms controlling tau filament formation can now be studied in yeast cells, in addition to allowing definition and testing of compounds and genes that inhibit or promote the process, while reducing the complexity of mammalian models for tauopathies, as for other disorders (*20*−*23*, *58*).

ACKNOWLEDGMENT

We thank Peter Davies for advice and for generous gifts of reagents.

REFERENCES

1. Goedert, M. (1996) Tau protein and the neurofibrillary pathology of Alzheimer's disease, *Ann. N.Y. Acad. Sci. 777*, 121−131.
2. Buée, L., Bussiére, T., Buée-Scherrer, V., Delacourte, A., and Hof, P. (2000) Tau protein isoforms, phosphorylation and role in neurodegenerative disorders, *Brain Res. Brain Res. Rev. 33*, 95−130.
3. Lee, V. M., Goedert, M., and Trojanowski, J. (2001) Neurodegenerative tauopathies, *Annu. Rev. Neurosci. 24*, 1121−1159.
4. Braak, H., and Braak, E. (1991) Neuropathological staging of Alzheimer-related changes, *Acta Neuropathol. (Berlin) 82*, 239−259.
5. Wang, J. Z., Gong, C. X., Zaidi, T., Grundke-Iqbal, I., and Iqbal, K. (1995) Dephosphorylation of Alzheimer paired helical filaments by protein phosphatase-2A and -2B, *J. Biol. Chem. 270*, 4854−4860.
6. Alonso, A., Zaidi, T., Novak, M., Grundke-Iqbal, I., and Iqbal, K. (2001) Hyperphosphorylation induces self-assembly of tau into tangles of paired helical filaments/straight filaments, *Proc. Natl. Acad. Sci. U.S.A. 98*, 6923−6928.
7. Zheng-Fischhöfer, Q., Biernat, J., Mandelkow, E. M., Illenberger, S., Godemann, R., and Mandelkow, E. (1998) Sequential phosphorylation of Tau by glycogen synthase kinase-3beta and protein kinase A at Thr212 and Ser214 generates the Alzheimer-specific epitope of antibody AT100 and requires a paired-helical-filament-like conformation, *Eur. J. Biochem. 252*, 542−552.
8. Abraha, A., Ghoshal, N., Gamblin, T. C., Cryns, V., Berry, R. W., Kuret, J., and Binder, L. I. (2000) C-terminal inhibition of tau assembly in vitro and in Alzheimer's disease, *J. Cell Sci. 113*, 3737−3745.
9. Weaver, C. L., Espinoza, M., Kress, Y., and Davies, P. (2000) Conformational change as one of the earliest alterations of tau in Alzheimer's disease, *Neurobiol. Aging 21*, 719−727.
10. Dou, F., Netzer, W. J., Tanemura, K., Li, F., Hartl, F. U., Takashima, A., Gouras, G. K., Greengard, P., and Xu, H. (2003) Chaperones increase association of tau protein with microtubules, *Proc. Natl. Acad. Sci. U.S.A. 100*, 721−726.
11. Shimura, H., Miura-Shimura, Y., and Kosik, K. S. (2004) Binding of tau to heat shock protein 27 leads to decreased concentration of hyperphosphorylated tau and enhanced cell survival, *J. Biol. Chem. 279*, 7957−7962.
12. Illenberger, S., Zheng-Fischhofer, Q., Preuss, U., Stamer, K., Baumann, K., Trinczek, B., Biernat, J., Godemann, R., Mandelkow, E. M., and Mandelkow, E. (1998) The endogenous and cell cycle-dependent phosphorylation of tau protein in living cells: implications for Alzheimer's disease, *Mol. Biol. Cell 9*, 1495−1512.
13. Smith, D. S., and Tsai, L. H. (2002) Cdk5 behind the wheel: a role in trafficking and transport?, *Trends Cell Biol. 12*, 28−36.
14. Terwel, D., Dewachter, I., and Van Leuven, F. (2002) Axonal transport, tau protein, and neurodegeneration in Alzheimer's disease, *Neuromol. Med. 2*, 151−165.
15. Doble, B. W., and Woodgett, J. R. (2003) GSK-3: tricks of the trade for a multi-tasking kinase, *J. Cell Sci. 116*, 1175−1186.
16. Liu, F., Iqbal, K., Grundke-Iqbal, I., and Gong, C. X. (2002) Involvement of aberrant glycosylation in phosphorylation of tau by cdk5 and GSK-3beta, *FEBS Lett. 530*, 209−214.
17. Bian, F., Nath, R., Sobocinski, G., Booher, R. N., Lipinski, W. J., Callahan, M. J., Pack, A., Wang, K. K., and Walker, L. C. (2002) Axonopathy, tau abnormalities, and dyskinesia, but no neurofibrillary tangles in p25-transgenic mice, *J. Comp. Neurol. 44*, 257−266.
18. Van den Haute, C., Spittaels, K., Van Dorpe, J., Lasrado, R., Vandezande, K., Laenen, I., Geerts, H., and Van Leuven, F. (2001) Coexpression of human cdk5 and its activator p35 with human protein tau in neurons in brain of triple transgenic mice, *Neurobiol. Dis. 8*, 32−44.
19. Hallows, J. L., Chen, K., DePhino, R. A., and Vincent, I. (2003) Decreased cyclin-dependent kinase 5 (cdk5) activity is accompanied by redistribution of cdk5 and cytoskeletal proteins and increased cytoskeletal protein phosphorylation in p35 null mice, *J. Neurosci. 23*, 10633−10644.
20. Edbauer, D., Winkler, E., Regula, J. T., Pesold, B., Steiner, H., and Haass, C. (2003) Reconstitution of gamma-secretase activity, *Nat. Cell Biol. 5*, 486−488.
21. Sherman, M. Y., and Muchowski, P. J. (2003) Making yeast tremble: yeast models as tools to study neurodegenerative disorders, *Neuromol. Med. 4*, 33−46.
22. Middendorp, O., Ortler, C., Neumann, U., Paganetti, P., Luthi, U., and Barberis, A. (2004) Yeast growth selection system for the identification of cell-active inhibitors of beta-secretase, *Biochim. Biophys. Acta 6*, 29−39.
23. Outeiro, T. F., and Muchowski, P. J. (2004) Molecular genetics approaches in yeast to study amyloid diseases, *J. Mol. Neurosci. 23*, 49−60.
24. Huang, D., Patrick, G., Moffat, J., and Tsai, L. H., and Andrews, B. (1999) Mammalian Cdk5 is a functional homologue of the budding yeast Pho85 cyclin-dependent protein kinase, *Proc. Natl. Acad. Sci. U.S.A. 96*, 14445−14450.
25. Nishizawa, M., Kanaya, Y., and Toh-E, A. (1999) Mouse cyclin-dependent kinase (Cdk) 5 is a functional homologue of a yeast Cdk, pho85 kinase, *J. Biol. Chem. 274*, 33859−33862.
26. Terwel, D., Lasrado, R., Snauwaert, J., Vandeweert, E., Van Haesendonck, C., Borghgraef, P., and Van Leuven, F. (2005) Changed conformation of mutant tau-P301L underlies the moribund tauopathy, absent in progressive, non-lethal axonopathy of tau-4R/2N transgenic mice, *J. Biol. Chem. 280*, 3963−3973.
27. Brachmann, C. B., Davies, A., Cost, G. J., Caputo, E., Li, J., Hieter, P., and Boecke, J. D. (1998) Designer deletion strains derived from *Saccharomyces cerevisiae* S288C: a useful set of strains and plasmids for PCR-mediated gene disruption and other applications, *Yeast 14*, 115−132.
28. Wallis, J. W., Chrebet, G., Brodsky, G., Rolfe, M., and Rothstein, R. (1989) A hyper-recombination mutation in *S. cerevisiae* identifies a novel eukaryotic topoisomerase, *Cell 58*, 409−419.
29. Wach, A., Brachat, A., Pohlmann, R., and Philippsen, P. (1994) New heterologous modules for classical or PCR-based gene disruptions in *Saccharomyces cerevisiae*, *Yeast 10*, 1793−1808.
30. Spittaels, K., Van den Haute, C., Van Dorpe, J., Bruynseels, K., Vandezande, K., Laenen, I., Geerts, H., Mercken, M., Sciot, R., Van Lommel, A., Loos, R., and Van Leuven, F. (1999) Prominent axonopathy in the brain and spinal cord of transgenic mice overexpressing four-repeat human tau protein, *Am. J. Pathol. 155*, 2153−2165.
31. Andoh, T., Hirata, Y., and Kikuchi, A. (2000) Yeast glycogen synthase kinase-3 activates Msn2p-dependent transcription of stress responsive genes, *Mol. Cell. Biol. 20*, 6712−6720.
32. Guldener, U., Heck, S., Fiedler, T., Beinhauer, J., and Hegemann, J. (1996) A new efficient gene disruption cassette for repeated use in budding yeast, *Nucleic Acids Res. 24*, 2519−2524.
33. Gietz, D., St. Jean, A., Woods, R. A., and Schiestl, R. M. (1992) Improved method for high efficiency transformation of intact yeast cells, *Nucleic Acids Res. 20*, 1425−1431.
34. Kaiser, C., Michaelis, S., and Mitchell, A. (1994) *Methods in yeast genetics*, Cold Spring Harbor Press, Cold Spring Harbor, New York.
35. Spittaels, K., Van den Haute, C., Van Dorpe, J., Geerts, H., Mercken, M., Bruynseels, K., Lasrado, R., Vandezande, K., Laenen, I., Boon, T., Van Lint, J., Vandenheede, J., Moechars, D., Loos, R., and Van Leuven, F. (2000) Glycogen synthase kinase-3beta phosphorylates protein tau and rescues the axonopathy in the central nervous system of human four-repeat tau transgenic mice, *J. Biol. Chem. 275*, 41340−41349.

36. Scott, C. W., Spreen, R. C., Herman, J. L., Chow, F. P., Davison, M. D., Young, J., and Caputo, C. B. (1993) Phosphorylation of recombinant tau by cAMP-dependent protein kinase. Identification of phosphorylation sites and effect on microtubule assembly, *J. Biol. Chem. 268*, 1166−1173.
37. Jicha, G. A., Weaver, C., Lane, E., Vianna, C., Kress, Y., Rockwood, J., and Davies, P. (1999) cAMP-dependent protein kinase phosphorylations on tau in Alzheimer's disease, *J. Neurosci. 19*, 7486−7494.
38. Uboga, N. V., and Price, J. L. (2000) Formation of diffuse and fibrillar tangles in aging and early Alzheimer's disease, *Neurobiol. Aging 21*, 1−10.
39. Nuydens, R., Van Den Kieboom, G., Nolten, C., Verhulst, C., Van Osta, P., Spittaels, K., Van den Haute, C., De Feyter, E., Geerts, H., and Van Leuven, F. (2002) Coexpression of GSK-3beta corrects phenotypic aberrations of dorsal root ganglion cells, cultured from adult transgenic mice overexpressing human protein tau, *Neurobiol. Dis. 9*, 38−48.
40. Sato, S., Tatebayashi, Y., Akagi, T., Chui, D. H., Murayama, M., Miyasaka, T., Planel, E., Tanemura, K., Sun, X., Hashikawa, T., Yoshioka, K., Ishiguro, K., and Takashima, A. (2002) Aberrant tau phosphorylation by glycogen synthase kinase-3beta and JNK3 induces oligomeric tau fibrils in COS-7 cells, *J. Biol. Chem. 277*, 42060−42065.
41. Carmel, G., Mager, E. M., Binder, L. I., and Kuret, J. (1996) The structural basis of Mab Alz50's selectivity for Alzheimer's disease pathology, *J. Biol. Chem. 271*, 32789−32795.
42. Rissman, R. A., Poon, W. W., Blurton-Jones, M., Oddo, S., Torp, R., Vitek, M. P., LaFerla, F. M., Rohn, T. T., and Cotman, C. W. (2004) Caspase-cleavage of tau is an early event in Alzheimer disease tangle pathology, *J. Clin. Invest. 114*, 121−130.
43. Puziss, J. W., Hardy, T. A., Johnson, R. B., Roach, P. J., and Hieter, P. (1994) MDS1, a dosage suppressor of an mck1 mutant, encodes a putative yeast homologue of glycogen synthase kinase 3, *Mol. Cell. Biol. 14*, 831−839.
44. Carrol, A. S., and O'Shea, E. K. (2002) Pho85 and signalling environmental conditions, *Trends Biochem. Sci. 27*, 87−93.
45. Wilson, W. A., and Roach, P. J. (2002) Nutrient-regulated protein kinases in budding yeast, *Cell 111*, 155−158.
46. Huang, D., Moffat, J., and Andrews B. (2002) Dissection of a complex phenotype by functional genomics reveals roles for the yeast cyclin-dependent protein kinase Pho85 in stress adaptation and cell integrity, *Mol. Cell. Biol. 22*, 5076−5088.
47. Carrol, A. S., Bishop, A. C., DeRisi, E. L., Shokat, K. M., and O'Shea, E. K. (2001) Chemical inhibition of the Pho85 cyclin-independent kinase reveals a role in the environmental stress response, *Proc. Natl. Acad. Sci. U.S.A. 98*, 12578−12583.
48. Gillardon, F., Schrattenholz, A., and Sommer, B. (2005) Investigating the neuroprotective mechanism of action of a CDK5 inhibitor by phosphoproteome analysis, *J. Cell. Biochem. 95*, 817−826.
49. Tan, Y. S., Morcos, P. A., and Cannon, J. F. (2003) Pho85 phosphorylates the Glc7 protein phosphatase regulator Glc8 in vivo, *J. Biol. Chem. 278*, 147−153.
50. Morfini, G., Szebenyi, G., Brown, H., Pant, H. C., Pigino, G., DeBoer, S., Beffert, U., and Brady, S. T. (2004) A novel CDK5-dependent pathway for regulating GSK3 activity and kinesin-driven motility in neurons, *EMBO J. 23*, 2235−2245.
51. Kadota, J., Yamamoto, T., Yoshiuchi, S., and Tanaka, K. (2004) Septin ring assembly requires concerted action of polarisome components, a PAK kinase Cla4p, and the actin cytoskeleton in *Saccharomyces cerevisiae*, *Mol. Biol. Cell 15*, 5329−5345.
52. Marquitz, A. R., Harrison, J. C., Bose, I., Zyla, T. R., McMillan, J. N., and Lew, D. J. (20??) The Rho-GAP Bem2p plays a GAP-independent role in the morphogenesis checkpoint, *EMBO J. 21*, 4012−4025.
53. Barghorn, S., and Mandelkow, E. (2002) Toward a unified scheme for the aggregation of tau into Alzheimer paired helical filaments, *Biochemistry 41*, 14885−14896.
54. Gamblin, T. C., Berry, R. W., and Binder, L. I. (2003) Modelling tau polymerization in vitro: a review and synthesis, *Biochemistry 42*, 15009−15017.
55. Chirita, C. N., and Kuret, J. (2004) Evidence for an intermediate in tau filament formation, *Biochemistry 43*, 1704−1714.
56. Zhang, W., Needham, D. L., Coffin, M., Rooker, A., Hurban, P., Tanzer, M. M., and Shuster, J. R. (2003) Microarray analyses of the metabolic responses of *Saccharomyces cerevisiae* to organic solvent dimethyl sulfoxide, *J. Ind. Microbiol. Biotechnol. 30*, 57−69.
57. Heutink, P. (2000) Untangling tau-related dementia, *Hum. Mol. Genet. 9*, 979−986.
58. Lindquist, S., Krobitsch, S., Li, L., and Sondheimer, N. (2001) Investigating protein conformation-based inheritance and disease in yeast, *Philos. Trans. R. Soc. London, Ser. B 356*, 69−76.

BI0506775